Phase-controlled pulse propagation in media with cross coupling of electric and magnetic probe field component

Robert Fleischhaker* and Jörg Evers†
Max-Planck-Institut für Kernphysik, Saupfercheckweg 1, D-69117 Heidelberg, Germany
(Received 29 June 2009; published 8 December 2009)

Light propagation is discussed in media with a cross coupling of the electric and magnetic component of an applied probe field. We derive the wave equations for a probe pulse propagating through such a medium and solve them analytically in Fourier space using the slowly varying envelope approximation. Our analysis reveals the influence of the different medium response coefficients on the propagation dynamics. We apply these results to a specific example system in which cross couplings are induced in an atomic medium by additional control fields. We show that the cross couplings render the propagation dynamics sensitive to the relative phase of the additional fields, and this phase dependence enables one to control the pulse during its propagation through the medium. Our results demonstrate that the magnetic field component of a probe beam can crucially influence the system dynamics already at experimentally accessible parameter ranges in dilute vapors.

DOI: 10.1103/PhysRevA.80.063816 PACS number(s): 42.50.Gy, 42.65.Sf, 42.65.An

I. INTRODUCTION

Quantum optics describes the interaction of matter and light at the quantum level [1,2]. In many cases, the underlying principles can already be understood from a fairly simple analysis, focusing on single atoms interacting with the electric field component of the driving laser fields. But recently, motivated by the aim of achieving a negative index of refraction in atomic media [3–7], a qualitatively different class of setups received a considerable amount of interest. The key feature of these setups is that a probe beam interacts with the medium both with its electric and its magnetic field component at the same time. Only if both the magnetic and the electric response are suitable, a negative refractive index (NRI) can be achieved. Related to the need for a high magnetic response, these systems have two more distinct features in common. First, they operate at a high density such that the different atoms in the medium are no longer independent [8–10]. Second, in order to enable a certain enhancement mechanism for the magnetic response, the laser fields couple to the medium in such a way that a cross coupling between the electric and magnetic probe field component is induced [6,11,12]. Unfortunately, an experimental implementation of these schemes to achieve atomic NRI media is very challenging. For example, suitable atomic species are rare and the required high density implies a number of problems such as Doppler broadening, radiation trapping [13,14], dephasing, or unwanted nonlinear processes.

It is important to note, however, that these challenges to a large degree arise from the specific requirements for NRI media. But the two key ingredients, high density and cross coupling of the electric and magnetic field, are of interest in their own rights. This raises the question whether it is possible to study the effects of density or cross coupling individually at much more accessible parameter ranges. It turns out that the answer is affirmative. Regarding experiments at high density, potential model systems could be, e.g., Rydberg-atoms, doped crystals, or cold gases. In a previous work, we studied dipole-dipole interactions in an electromagnetically induced transparency setup at high density [15]. We could show that the polarization contribution to the local field strongly modulates the phase of a weak probe pulse. It was found that this phase modulation distinctively differs from the nonlinear self-phase modulation experienced by a strong pulse in a Kerr medium.

Here, we turn to the second key ingredient of NRI schemes and analyze light propagation in a dilute sample of atoms with field-induced cross coupling of the electric and magnetic probe field component. Quantum optical setups routinely neglect the magnetic field components of the applied electromagnetic fields altogether. Generally, this is justified due to the weak interaction strength and since magnetic transitions are typically off-resonant from the applied fields. Interestingly, a complete switch from electric to magnetic dipole transitions would not change the obtained results qualitatively, as the structure of the system Hamiltonian is essentially unchanged. It is only the combination of magnetic and electric field interactions in a cross coupling setup that gives rise to different results.

We start by solving the wave equations in slowly varying envelope approximation (SVEA) for an arbitrary medium with a cross coupling of the electric and magnetic field. Our solution allows to understand the influence of the different response coefficients that characterize light propagation in such a medium. In a next step, we discuss the necessary conditions to implement an atomic medium with a cross coupling. Based on these results, we analyze an example system in which a cross coupling is induced in an atomic medium by additional control fields. We study light propagation through this medium and find that the cross coupling becomes relevant already at low medium density. It gives rise to a sensitivity of the system dynamics to the relative phase of the additional fields. We show that this dependence can be used to control the propagation dynamics of the probe pulse, even throughout the pulse propagation. The results are interpreted based on our analytical solution and all conclusions are veri-

*robert.fleischhaker@mpi-hd.mpg.de
†joerg.evers@mpi-hd.mpg.de

fied using a full numerical solution of the propagation equations.

In a broader context, our results demonstrate that the magnetic field component of the probe field can crucially influence the propagation dynamics of the light pulse, even though it couples to the medium only very weakly. This may pave the way to further applications of *magnetic quantum optics*, utilizing both electric and magnetic components of the applied laser fields. Also, it will turn out that the analysis of media with cross coupling sheds light on the related so-called closed-loop systems [16,17]. We will find that media with a field-induced cross coupling are an ideal implementation of a closed-loop phase-control scheme for light propagation.

The paper is structured as follows. In Sec. II, we define media with a cross coupling of the electric and magnetic field component in terms of a macroscopic electrodynamic description and discuss their linear response. The following Sec. III analyzes light propagation in such media. In particular, we analytically solve the corresponding wave equations in SVEA. The following Sec. IV discusses possible implementations of media with a cross coupling in atomic systems. Based on these results, we discuss light propagation in a concrete model system in Sec. V, with the emphasis on phase control of the propagation dynamics. Section VI discusses and summarizes the results.

II. CROSS COUPLING OF THE ELECTRIC AND MAGNETIC FIELD

In quantum optical calculations, usually the direct interaction of the magnetic component of applied laser fields with the atoms is neglected [18]. This is because typically, the laser field is not in resonance with magnetic dipole transitions and the magnetic response is parametrically suppressed by two powers of the fine structure constant α compared to the electric response. To see this, we consider a homogeneous isotropic medium. The linear response coefficients to the electric field $\mathbf{E}$ and the magnetizing field $\mathbf{H}$ are then given by [19]

$$\mathbf{P}(t) = \int \varepsilon_0 \chi_E(\tau)\mathbf{E}(t-\tau)d\tau, \tag{1a}$$

$$\mathbf{M}(t) = \int \chi_H(\tau)\mathbf{H}(t-\tau)d\tau, \tag{1b}$$

with polarization $\mathbf{P}$, magnetization $\mathbf{M}$, and ε_0 the permittivity of free space. The coefficients χ_E and χ_H account for the direct response of the medium to the electric and magnetic field. Magnetic dipole matrix elements are suppressed by one power of the fine structure constant,

$$m/d \sim \alpha c \Rightarrow |mB| \sim \alpha |dE|, \tag{2}$$

with magnetic dipole moment m, magnetic field B, electric dipole moment d, and electric field E. A direct response involves the dipole coupling twice, first when the field induces a dipole moment and once more when the induced dipole moment couples back to the field. Therefore, the direct magnetic response in comparison to the direct electric response is suppressed by two powers of the fine structure constant,

$$\chi_H \sim \alpha^2 \chi_E. \tag{3}$$

This weak coupling of the magnetic field component can be partially remedied in a more general medium [6,11,20], which is described by response functions

$$\mathbf{P}(t) = \int \varepsilon_0 \chi_E(\tau)\mathbf{E}(t-\tau) + \frac{1}{c}\xi_{EH}(\tau)\mathbf{H}(t-\tau)d\tau, \tag{4a}$$

$$\mathbf{M}(t) = \int \chi_H(\tau)\mathbf{H}(t-\tau) + \frac{1}{c\mu_0}\xi_{HE}(\tau)\mathbf{E}(t-\tau)d\tau, \tag{4b}$$

with μ_0 the permeability of free space and $c=1/\sqrt{\varepsilon_0\mu_0}$ the speed of light in vacuum. The two additional coefficients ξ_{EH} and ξ_{HE} account for a cross coupling of the electric and magnetic field component, in the sense that the electric field induces magnetization and the magnetic field induces polarization. Such a cross coupling leads to a parametric enhancement of the magnetic response by a factor of α^{-1} [11], since it involves only one magnetic dipole coupling,

$$\xi_{HE} \sim \alpha\chi_E \quad \text{and} \quad \xi_{HE} \sim \alpha^{-1}\chi_H. \tag{5}$$

It is because of this enhancement of the magnetic response that such cross couplings of the electric and magnetic field have been considered for the realization of a negative index of refraction in atomic gases.

A further consequence of a cross coupling of electric and magnetic field concerns the transformation properties of the medium. In Eqs. (4), we have assumed simple, nontensorial response coefficients. Since ξ_{EH} and ξ_{HE} in Eqs. (4) each relate a polar vector $(\mathbf{P},\mathbf{E})$ to an axial vector $(\mathbf{M},\mathbf{H})$, they are pseudoscalars. Hence, they change sign under space inversion such that the electrodynamic response properties change. It turns out that this assumption can be realized, e.g., if the probing light field is circularly polarized in the $x-y$ plane and propagates in $\pm z$ direction [6,7]. These transformation properties are similar to the case of chiral molecules which exhibit a different optical activity depending on the enantiomer. Indeed, in the design of metamaterials a chiral structure of the conducting elements can be used to induce a cross coupling [11,21,22]. Regarding their symmetry, chiral media constitute a subclass of media with cross couplings characterized by $\xi_{EH}=-\xi_{HE}$ [23–25]. The atoms considered here differ from conventional, inherently chiral media in that the cross couplings typically have to be induced by external control fields. It is thus the atoms together with the control fields which form the effective medium. Depending on the implementation of the control fields and on the atomic structure, it may not be possible to probe the same effective medium with light of different circular polarization, thereby directly verifying the difference in optical activity for different polarizations.

III. LIGHT PROPAGATION

In this section, we derive the wave equations for the electric and magnetic field components of a probe field taking

into account a cross coupling of the field components. This is in contrast to the usual treatment in which a coupling to only the electric component is assumed. We apply the SVEA in order to transform the second order wave equations to equations involving first order derivatives only. Using Fourier transformation techniques, we find the general solution to the first order wave equations and compare the result to the index of refraction obtained from a single particle susceptibility analysis.

A. Wave equations for the electric and the magnetic field components

As a basis for our following analysis, we start from the two inhomogeneous macroscopic Maxwell's equations [19],

$$\nabla \times \mathbf{E} = -\partial_t \mathbf{B}, \tag{6a}$$

$$\nabla \times \mathbf{H} = \partial_t \mathbf{D}, \tag{6b}$$

with the electric field **E**, the magnetic field **B**, the electric displacement field **D**, and the magnetizing field **H**. The medium is described by its polarization **P** and magnetization **M** which are related to the quantities entering the Maxwell's equations via the constitutive relations

$$\mathbf{D} = \varepsilon_0 \mathbf{E} + \mathbf{P}, \tag{7a}$$

$$\mathbf{H} = \frac{1}{\mu_0}\mathbf{B} - \mathbf{M}. \tag{7b}$$

We do not consider the two homogeneous Maxwell's equations since with no external sources or currents and assuming transverse fields they are always fulfilled.

From Eqs. (6) and (7), we can derive wave equations for the electric and magnetic field,

$$\left[\Delta - \frac{1}{c^2}\partial_t^2\right]\mathbf{E} = \mu_0 \partial_t^2 \mathbf{P} + \mu_0 \partial_t \nabla \times \mathbf{M}, \tag{8a}$$

$$\left[\Delta - \frac{1}{c^2}\partial_t^2\right]\mathbf{B} = \mu_0 \Delta \mathbf{M} - \mu_0 \partial_t \nabla \times \mathbf{P}, \tag{8b}$$

with sources given by the polarization and magnetization of the medium. In the following, we specialize to the case of a one-dimensional propagation. We choose the positive z axis as the propagation direction and separate a complex envelope function $X_0(z,t)$ from the carrier wave,

$$\mathbf{X} = \frac{1}{2} X_0(z,t)\mathbf{e}_{\pm} e^{i(k_0 z - \omega_0 t)} + \text{c.c.}, \tag{9}$$

where **X** stands for **E**, **B**, **P**, or **M**. The complex unit vector for left-or right-circular polarized light is $\mathbf{e}_{\pm}$, and the wave number of the carrier wave in vacuum is k_0 with $\omega_0 = ck_0$ as the corresponding frequency. Assuming that variations in space and time of the envelope function are on a much larger scale than the wavelength $\lambda_0 = 2\pi/k_0$ and the oscillation period $T_0 = 2\pi/\omega_0$ of the carrier wave, we can apply the SVEA [1]. In this approximation derivatives of the envelope function in space and time are neglected compared to derivatives of the carrier wave. As a consequence, SVEA reduces the wave equations Eqs. (8) to first order equations for the envelope functions,

$$\left[\partial_z + \frac{1}{c}\partial_t\right] E_0(z,t) = \frac{ik_0}{2\varepsilon_0} P_0(z,t) \mp \frac{k_0}{2\varepsilon_0 c} M_0(z,t), \tag{10a}$$

$$\left[\partial_z + \frac{1}{c}\partial_t\right] B_0(z,t) = \frac{ik_0\mu_0}{2} M_0(z,t) \pm \frac{k_0}{2\varepsilon_0 c} P_0(z,t). \tag{10b}$$

In the following, the upper sign applies for left-circular polarization whereas the lower sign applies for right-circular polarization. Eqs. (10) are considerably simpler to solve analytically as well as numerically than the second order Eqs. (8) we derived initially. Yet, they still incorporate the essential physics of light propagation in one dimension for a medium with a cross coupling of the electric and the magnetic component of a weak probe field.

B. Solution of the wave equations

We will now solve the wave Eqs. (10) to a level that enables us to determine how the actual propagation dynamics depends on the four quantities χ_E, χ_H, ξ_{EH}, and ξ_{HE} characterizing the medium. First, we transform Eqs. (10) into Fourier space. To substitute P_0 and M_0 we also Fourier transform Eqs. (4) and to replace H_0 by B_0 we use the Fourier transform of Eq. (7b). Finally, we can combine both wave equations into a single matrix equation for the vector $\mathbf{F}(z,t) = [E_0(z,t), cB_0(z,t)]^T$,

$$\partial_z \mathbf{F}(z,\Delta_p) = ik_0 \mathcal{M} \mathbf{F}(0,\Delta_p), \tag{11}$$

and the elements of the matrix $\mathcal{M}$ are given by

$$\mathcal{M}_{1,1} = \frac{\Delta_p}{\omega_o} + \frac{1}{2\mu}(\chi_E - \xi_{EH}\xi_{HE} \pm i\xi_{HE}), \tag{12a}$$

$$\mathcal{M}_{1,2} = \frac{1}{2\mu}(\xi_{EH} \pm i\chi_H), \tag{12b}$$

$$\mathcal{M}_{2,1} = \frac{1}{2\mu}(\xi_{HE} \mp i\mu\chi_E \pm i\xi_{EH}\xi_{HE}), \tag{12c}$$

$$\mathcal{M}_{2,2} = \frac{\Delta_p}{\omega_0} + \frac{1}{2\mu}(\chi_H \pm i\xi_{EH}). \tag{12d}$$

In these equations, the detuning $\Delta_p = \omega - \omega_0$ accounts for the frequency distribution of the envelope functions around the carrier frequency. Applying the vacuum phase relation for circularly polarized light, $cB_0 = \mp iE_0$, we find that the initial condition for the evolution,

$$\mathbf{F}(0,\Delta_p) = \begin{pmatrix} E_0(0,\Delta_p) \\ \mp iE_0(0,\Delta_p) \end{pmatrix}, \tag{13}$$

is an eigenvector to matrix $\mathcal{M}$ in Eq. (11). Therefore, the solution can be calculated with the help of the corresponding eigenvalue η. The solution reads

$$\mathbf{F}(z,\Delta_p) = e^{ik_0\eta z}\begin{pmatrix} E_0(0,\Delta_p) \\ \mp iE_0(0,\Delta_p) \end{pmatrix}, \tag{14}$$

and the frequency dependence is contained in the eigenvalue

$$\eta = \frac{\Delta_p}{\omega_0} + \frac{1}{2\mu}[\chi_E\mu + \chi_H - \xi_{EH}\xi_{HE} \mp i(\xi_{EH} - \xi_{HE})]. \tag{15}$$

This result can be compared to the refractive index in a medium with a cross coupling which on the basis of Eqs. (4) was shown to evaluate to [6]

$$n_\pm = \sqrt{\varepsilon\mu - \frac{1}{4}(\xi_{EH} + \xi_{HE})^2} \mp \frac{i}{2}(\xi_{EH} - \xi_{HE}). \tag{16}$$

Here, $\varepsilon = 1 + \chi_E$ and $\mu = 1 + \chi_H$. The upper sign applies for left-circularly polarized light and the lower sign for right-circularly polarized light. The application of SVEA is equivalent to the condition $|n_\pm - 1| \ll 1$, such that we can perform a first-order Taylor expansion of the square root contribution in Eq. (16). Keeping terms linear in the response coefficients we find

$$n_\pm = 1 + \frac{1}{2}(\chi_E + \chi_H) \mp \frac{i}{2}(\xi_{EH} - \xi_{HE}). \tag{17}$$

Linearizing Eq. (15) and taking into account the contribution of the carrier wave, we find the same result as in Eq. (17). This demonstrates the consistency of our solution with the previously calculated index of refraction. Our result based on the solution of the wave equations, however, has the advantage that it offers the possibility to study propagation dynamics. Because of the simple formulas we have derived, analytical solutions become accessible. If for a specific system the frequency dependencies of χ_E, χ_H, ξ_{EH}, and ξ_{HE} are known, it can be used together with the solution in frequency domain Eq. (14) to calculate the actual dynamics in time domain.

IV. IMPLEMENTATION OF CROSS COUPLINGS IN ATOMIC MEDIA

In this section we discuss the general conditions for realizing an atomic medium with response in the form of Eqs. (4), as introduced in Sec. II. As a first condition, a medium in addition to an electric probe field transition should exhibit a near-degenerate transition coupling to the magnetic component of the probe field. A second condition is that, to enable cross couplings, there must be a mechanism to allow for polarization (magnetization) to be induced by the magnetic (electric) probe field component.

The first condition can be difficult to fulfill in atomic media. A small frequency difference between electric and magnetic probe field transition could be removed by an external magnetic field leading to a Zeeman shift, but magnetic dipole transitions are usually found in a much smaller frequency range compared to electric dipole transitions. The reason is that due to selection rules imposed by the corresponding transition matrix element, magnetic dipole transitions can only occur between states of the same parity. This implies that magnetic dipole transitions only take place between states with the same angular momentum quantum number whereas electric dipole transitions connect states of different angular momentum. A possible solution are atomic species with a large spin-orbit coupling [26]. Then, states with the same angular momentum quantum number can display a large splitting and their transition frequency can become comparable to the transition frequency of an electric dipole transition. This could also help to realize a probe field transition frequency in the optical domain which is especially attractive for applications. Motivated by ideas like NRI, several atomic species have been investigated with respect to this condition. Dysprosium [6,27], hydrogen [4], metastable neon and other noble gases [4,28] have been identified as promising candidates. An alternative approach could be to make use of nonresonant two-photon transitions in order to relax the requirement of having both electric and magnetic transitions at similar transition frequencies [7,28].

The second condition can be implemented in closed-loop systems. In these systems the laser-driven transitions form a closed interaction contour such that photon emission and absorption can take place in a cycle [16,17,29–41]. Because the closed interaction contour enables quantum mechanical pathway interference, it can render the system phase dependent. It should be noted that in general, a specific control field setup only gives rise to a closed-loop configuration for a single probe field polarization, whereas a different polarization would require another implementation of the control fields. This is a difference of field-induced and inherent cross couplings. Closed-loop systems have mainly been investigated in contexts where the closed interaction contour only includes the coupling to one (electric) probe field component [17,31–36]. This is known to induce extra contributions to the medium response, but these cannot be utilized for light propagation of a pulsed probe field in a straightforward way [37,38]. The reason is that already without the probe field such a configuration would give rise to parametric processes which scatter the control fields into the probe field mode [37–41]. As we will see in Sec. V, this conclusion changes in the case of a closed-loop system including both the electric and magnetic probe field component. There, we will find that the closed-loop phase can provide a convenient control parameter for light propagation in such media.

V. PHASE CONTROL OF PROPAGATION DYNAMICS

A. Model system

In this section, we apply the results obtained so far to discuss light propagation in a specific system with simultaneous coupling to the electric and the magnetic component of a probe laser field. The atomic medium is modeled by the five level scheme shown in Fig. 1. It was first introduced in the context of generating atomic media exhibiting a negative index of refraction [6]. In zeroth order of the probe field, the atomic medium forms an effective three-level system in Λ configuration consisting of states $|1\rangle$, $|4\rangle$, and $|5\rangle$. Two strong resonant control fields with Rabi frequencies Ω_1 and Ω_2 prepare the atoms in a dark state, i.e., a stable coherent superposition of states $|1\rangle$ and $|4\rangle$. The magnetic and electric probe field components couple to degenerate magnetic and electric

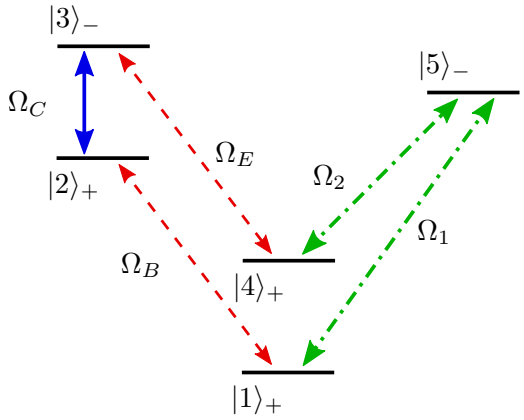

FIG. 1. (Color online) Atomic level scheme used to describe the medium. Two strong control fields with Rabi frequencies Ω_1 and Ω_2 prepare a coherent superposition of states $|1\rangle$ and $|4\rangle$. The magnetic and electric probe beam components couple to two transitions with Rabi frequencies Ω_B and Ω_E, respectively. Ω_C describes an additional control field. A possible combination of relative state parities is denoted by the + and − labels.

dipole transitions with Rabi frequencies Ω_B and Ω_E, and the upper levels of these two dipole transitions are coupled by an additional resonant control field with Rabi frequency Ω_C. We assume that state $|1\rangle$ and $|4\rangle$ have the same parity. Because the electric probe field transition couples states of different parity whereas the magnetic probe field transition couples states of the same parity, the additional control field couples to an electric dipole transition. Note that the Rabi frequencies $\Omega_i=|\Omega_i|\exp[i(\vec{k}_i\cdot\vec{r}+\varphi_i)]$ are complex, and contain the wave vector $\vec{k}_i$ and the absolute phase φ_i ($i\in\{1,2,C,E,B\}$).

As discussed in Sec. II, the linear response of the atomic medium is characterized by two contributions. First, direct contributions arise from the polarization (magnetization) induced by the electric (magnetic) probe field component. The other contributions to the medium response are the cross couplings, which arise due to polarization (magnetization) induced by the magnetic (electric) probe field component. It was found that the considered level scheme displays a relevant magnetic response due to these cross contributions [6,20]. Apart from the enhancement by α^{-1}, the magnetic response is proportional to the strength of the ground state coherence of state $|1\rangle$ and $|4\rangle$ and the control field Ω_C.

The Hamiltonian of the system in Fig. 1 in a suitable interaction picture is given by [1]

$$H_I=-\hbar\Delta_p(A_{22}+A_{33})-\frac{\hbar}{2}(\Omega_B A_{21}+\Omega_E A_{34}+\Omega_C A_{32}+\Omega_1 A_{51}+\Omega_2 A_{54}+\text{H.c.}), \tag{18}$$

where Δ_p is the probe field detuning and atomic transition operator is defined as $A_{jk}=|j\rangle\langle k|$. An interesting insight into the involved physics can be gained by applying a further unitary transformation to the Hamiltonian

$$\bar{H}_I=-\hbar\Delta_p(A_{22}+A_{33})-\frac{\hbar}{2}(|\Omega_B|A_{21}+|\Omega_E|A_{34}+|\Omega_C|e^{i\Phi}A_{32}+|\Omega_1|A_{51}+|\Omega_2|A_{54}+\text{H.c.}). \tag{19}$$

It can be seen that H_I contains a phase contribution

$$\Phi=(\varphi_2-\varphi_1+\varphi_c)+(\vec{k}_2-\vec{k}_1+\vec{k}_C)\vec{r}, \tag{20}$$

which cannot be removed entirely via unitary transformations. The origin of this phase dependence is the closed-loop structure of the considered level scheme. Starting from $|1\rangle$, the system can evolve in a nontrivial loop sequence $|1\rangle\rightarrow|5\rangle\rightarrow|4\rangle\rightarrow|3\rangle\rightarrow|2\rangle\rightarrow|1\rangle$ back to the initial state. This enables pathway interference, e.g., from $|1\rangle$ to $|3\rangle$ either via $|5\rangle$ and $|4\rangle$, or via $|2\rangle$. The phase difference between these two interfering pathways is equivalent to the phase difference given by Eqs. (19) and (20). It is interesting to note that the closed-loop phase Φ does not contain properties of the probe field, which is due to the fact that a closed transition loop involves both an absorption and an emission of a probe field photon. This property distinguishes the present scheme of all previous implementations of closed-loop media. Furthermore, Φ does not depend on time, because of the cancellation of the probe field and because the three control fields $\Omega_1,\Omega_2,\Omega_C$ are applied on resonance.

We are now also in the position to understand why a phase control of light propagation is possible in closed-loop media with a cross coupling between the electric and magnetic field component, in contrast to closed-loop media coupling only to the electric component of the probe field. From Fig. 1, it can be seen that in the presence of the probe field, a closed loop is established, such that the medium becomes sensitive to the closed-loop phase Φ. But in the absence of the probe field two transitions in the closed-loop structure are undriven. It follows that parametric processes scattering the control fields into the probe field mode cannot occur, independent of the phase matching condition assumed for the wave vectors of the probe and driving fields. This crucial difference to closed-loop media coupling to the electric probe field component only enables the phase control of light propagation that we will find in Sec. V B.

In the following, we continue our analysis based on the Hamiltonian H_I in Eq. (18) and assume that the laser configuration satisfies the usual phase matching condition $\vec{k}_2-\vec{k}_1+\vec{k}_C=1$, such that the system dynamics only depends on the relative phase

$$\Phi_0=\varphi_2-\varphi_1+\varphi_c. \tag{21}$$

In zeroth order of the probe fields, the equations of motion (EOM) governing the dynamics of the atomic degrees of freedom can easily be solved. The nonvanishing density matrix elements are

$$\rho_{11}^{(0)}=\frac{|\Omega_2|^2}{|\Omega_1|^2+|\Omega_2|^2}, \tag{22a}$$

$$\rho_{44}^{(0)}=\frac{|\Omega_1|^2}{|\Omega_1|^2+|\Omega_2|^2}, \tag{22b}$$

$$\rho_{41}^{(0)}=-\frac{\Omega_1\Omega_2^*}{|\Omega_1|^2+|\Omega_2|^2}. \tag{22c}$$

The linear response to a weak probe field does not disturb this dark state prepared by Ω_1 and Ω_2, and can thus be calculated on the basis of the lowest-order populations. To take

into account local field effects (LFC) in a dense gas a generalized form of the Clausius-Mossotti equation [19] has been used to numerically extract χ_E, χ_H, ξ_{EH}, and ξ_{HE} from the steady state solution to linear order in the local fields E_{loc} and B_{loc} in [6]. We pursue a different strategy here which provides us with an analytic solution including LFC [15]. We directly replace the local fields in the EOM by the external fields E_{ext} and B_{ext} with the help of the Lorenz-Lorentz relations

$$E_{\mathrm{loc}} = E_{\mathrm{ext}} + \frac{1}{3\varepsilon_0} P, \tag{23a}$$

$$B_{\mathrm{loc}} = B_{\mathrm{ext}} + \frac{\mu_0}{3} M. \tag{23b}$$

This leads to nonlinear EOM if the polarization P and the magnetization M are expressed by microscopic expectation values of the electric and magnetic dipole density containing elements of the atomic density matrix. Since we are interested in linear response, we expand the EOM up to linear order in the probe field and solve for the steady state. From this steady state solution, we find for the response coefficients

$$\chi_E = \frac{3L\gamma_{34}\rho_{44}^{(0)} \frac{i}{2}\Gamma_{24}}{\Gamma_{34}\Gamma_{24} + \frac{|\Omega_C|^2}{4}}, \tag{24a}$$

$$\chi_H = \frac{3L\gamma_{34}\alpha^2\rho_{11}^{(0)} \frac{i}{2}\Gamma_{31}}{\Gamma_{21}\Gamma_{31} + \frac{|\Omega_C|^2}{4}} \left(1 - \frac{\xi_{EH}|\rho_{41}^{(0)}| \frac{|\Omega_C|}{4} e^{-i\Phi_0}}{3\alpha\rho_{11}^{(0)} \frac{i}{2}\Gamma_{31}} \right), \tag{24b}$$

$$\xi_{EH} = \frac{3L\gamma_{34}\alpha|\rho_{41}^{(0)}| \frac{|\Omega_C|}{4}}{\Gamma_{34}\Gamma_{24} + \frac{|\Omega_C|^2}{4}} e^{i\Phi_0}, \tag{24c}$$

$$\xi_{HE} = \frac{3L\gamma_{34}\alpha|\rho_{41}^{(0)}| \frac{|\Omega_C|}{4}}{\Gamma_{21}\Gamma_{31} + \frac{|\Omega_C|^2}{4}} \left(1 + \frac{\chi_E}{3} \right) e^{-i\Phi_0}, \tag{24d}$$

where $L = N\lambda^3/4\pi^2$ includes the dependence on the number of particles $N\lambda^3$ per wavelength λ cubed. The decay rate and the detuning including the typical LFC shift for the electric and magnetic probe field transitions are given by

$$\Gamma_{34} = \gamma/2 + \gamma_{\mathrm{dec}} - i(\Delta_p + \rho_{44}^{(0)} L\gamma_{34}/2), \tag{25a}$$

$$\Gamma_{21} = \gamma_{21}/2 + \gamma_{\mathrm{dec}} - i\Delta_p, \tag{25b}$$

where $\gamma = \gamma_{31} + \gamma_{32} + \gamma_{34}$ is the overall decay rate of state $|3\rangle$ and γ_{dec} accounts for additional decoherence induced by atomic collisions.

Interpreting the dark state of $|1\rangle$ and $|4\rangle$ as a single quantum state characterized by the coherence between the two states, both probe field transitions can be viewed as being part of a three-level electromagnetically induced transparency (EIT) system [42,43]. The electric probe field and the control field Ω_C form a Λ system for which

$$\Gamma_{24} = \gamma_{21}/2 - i\Delta_p, \tag{26}$$

contains the ground-state decoherence and the two-photon detuning. No additional decoherence γ_{dec} besides the decay of the magnetic probe field transition has to be included if we assume that levels $|2\rangle$ and $|4\rangle$ are nearly degenerate, as then phase-perturbing collisions in the medium lead to random, but correlated phase shifts of the two states [6]. The magnetic probe field and the control field Ω_C form a ladder system in which the decoherence and two-photon detuning relevant for EIT is described by

$$\Gamma_{31} = \gamma/2 + 2\gamma_{\mathrm{dec}} - i\Delta_p. \tag{27}$$

By inspection of the structure of the solution for χ_E and χ_H, we find that the direct electric and magnetic responses of the EIT system are amended by LFC. The electric response features the usual EIT transparency window which is only degraded by a weak ground state decoherence given by γ_{21}, the linewidth of the magnetic probe field transition. The transparency window of the direct magnetic response on the other hand is not as prominent due to strong decoherence $\gamma/2 + 2\gamma_{\mathrm{dec}}$ in the ladder system. But this does not affect the propagation dynamics much since χ_H is suppressed by a factor α^2 compared to χ_E as discussed above. In particular for propagation dynamics at densities corresponding to $L \leq 1$, it can be neglected. On the contrary, the cross couplings are only suppressed by a factor of α and do influence the propagation dynamics. As expected, they are proportional to $|\rho_{41}^{(0)}|$, $|\Omega_C|$, and depend on the relative closed-loop phase Φ_0. From these solutions, we expect a propagation with a reduced group velocity and with a phase dependent refractive index induced by the cross couplings.

Two further observation about the cross coupling coefficients of the medium can be made. First, in the sense of a macroscopic electrodynamic description, the control fields Ω_C, Ω_1, and Ω_2 are part of the medium. Thus, they change sign when this effective medium is inverted and lead to the expected pseudoscalar behavior of ξ_{EH} and ξ_{HE} as described in Sec. II. Second, from Eq. (24) it follows in the limit $\Gamma_{ij} \ll |\Omega_C|$ and for dilute gases, that $\xi_{EH}/\xi_{HE} = \exp[2i\Phi_0]$. Thus, the closed-loop phase Φ_0 can be chosen such that the response coefficients approximately fulfill the condition $\xi_{EH} = -\xi_{HE}$ of a chiral medium.

With the analytic solution for χ_E, χ_H, ξ_{EH}, and ξ_{HE} at hand, we can now proceed to study propagation effects in the medium, focusing on control of the propagation dynamics via the closed-loop phase as concrete application.

B. Resulting propagation dynamics

In this section we study the propagation dynamics of a pulsed probe field in a medium as discussed in Sec. V A. Due to the direct electric response, the probe pulse propagates with a reduced group velocity, as it is the case in a usual EIT system. If we write the group velocity

$$v_g = \frac{c}{1+n_g}, \tag{28}$$

the group index n_g it is given by

$$n_g = \frac{3L\omega\gamma_{34}\rho_{44}^{(0)}}{|\Omega_C|^2}. \tag{29}$$

This is the standard expression in a EIT system, except for the scaling by the population fraction $\rho_{44}^{(0)}$ in the ground state of the electric probe field transition. The direct magnetic response can be neglected and all additional influence of the medium on a probe pulse is due to the cross coupling of the electric and magnetic probe field components.

The cross coupling is mediated by the closed interaction loop and depends on the relative phase Φ_0 between the three control fields. In contrast to the absolute phase, the relative phase of the applied fields can be controlled in an experiment (see e.g., [29,34,44]). Since the probe field propagates with strongly reduced group velocity whereas the control field Ω_C propagates at speed of light, a phase change in Φ_0 during the propagation of the probe pulse changes the frequency dependent refractive index for the probe field nearly instantaneously. In a similar fashion as a light pulse can be slowed down, stored, and retrieved by changing the amplitude of the control field [45], the phase of the control field can be used as a tool to control the refractive index for the probe pulse.

To clarify this idea further, in the following, we present two exemplary results from a numerical solution of the atomic EOM coupled to the wave equations for the two probe field components and the control field. We assume a medium with a density corresponding to $L=0.01$. For $\lambda = 795$ nm, this translates to $N \sim 8\times 10^{11}$ cm^{-3}. The control field strength is chosen as $|\Omega_C|=2\gamma$ and the dark state as symmetric, $|\Omega_1|=|\Omega_2|$, such that $\rho_{11}^{(0)}=\rho_{44}^{(0)}=0.5$ and $\rho_{41}^{(0)}=-0.5$. In both cases, we propagate a Gaussian probe pulse with a width in time of $\sigma=50/\gamma$. Its spectrum is well contained in the EIT transparency window such that it suffers very little absorption and broadening. We use a collisional decoherence of $\gamma_{\mathrm{dec}}=0.5\gamma$ and for the probe field we assume left-circular polarization.

In the first example, the phase Φ_0 is chosen constant as $\pi/2$. In Fig. 2, we show the corresponding propagation dynamics. The envelope of the electric probe field component is depicted for four successive propagation times, together with the real and imaginary part of the envelope and the pulse phase. The group velocity observed in the numerical calculation is consistent with Eqs. (28) and (29). We find that throughout the propagation, the phase of the pulse increases linearly. Thus, the real and imaginary parts of the envelope interchange while the absolute value of the envelope remains constant. This dynamics is due to a positive real index of refraction at resonance. Its theoretical value can be deduced

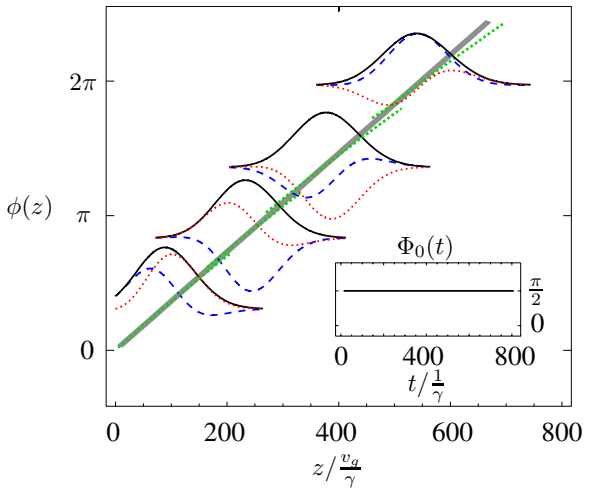

FIG. 2. (Color online) Propagation dynamics in a medium with cross coupling. The closed-loop phase $\Phi_0=\pi/2$ is kept constant, see inset. The absolute value (solid black lines), the real part (dashed blue lines), and the imaginary part (dotted red lines) of the probe pulse envelope are plotted for successive propagation times. Arbitrary, but consistent units are used and successive plots are vertically offset by the overall phase at the center of the pulse. The spatial phase dependence of each pulse (dashed green straight lines) is compared to the value expected from the analytical solution (thick gray straight line).

from the solutions given in Secs. III B and V. Neglecting χ_H, the eigenvalue Eq. (15) reduces to

$$\eta = \frac{\Delta_p}{\omega_0} + \frac{1}{2}[\chi_E - i(\xi_{EH} - \xi_{HE})]. \tag{30}$$

The term linear in Δ_p arising from χ_E leads to the reduced group velocity given in Eq. (28). We approximate ξ_{EH} and ξ_{HE} by the constant term at resonance leading to a constant refractive index. Fourier transforming Eq. (14) back into time domain, we find

$$\begin{pmatrix}\Omega_E(z,t)\\ \Omega_B(z,t)\end{pmatrix} = \begin{pmatrix}\Omega_E(0,t-z/v_g)\\ \Omega_B(0,t-z/v_g)\end{pmatrix} e^{i\beta k_0 z}, \tag{31}$$

in which the cross coupling part of the eigenvalue is given by

$$\beta = i\alpha\frac{n_g\rho_{41}^{(0)}|\Omega_C|}{2\omega\rho_{44}^{(0)}}\left(e^{i\Phi_0} - \frac{|\Omega_C|^2 e^{-i\Phi_0}}{2\gamma_{\mathrm{dec}}\gamma + 8\gamma_{\mathrm{dec}}^2 + |\Omega_C|^2}\right), \tag{32}$$

where we neglected the radiative decay of the magnetic probe field transition γ_{21} which is small compared to γ_{dec}.

Inserting the parameters chosen in Fig. 2, we obtain a positive real value of β such that the phase of the envelope increases constantly with propagation distance. In Fig. 2, we compare this phase dependence obtained from our approximate analytical model with the phase from the numerical propagation of the pulse at different propagation distances. At the center of the pulse the agreement between numerical and analytical solution is very good. Away from the center there are small deviations that increase with propagation distance. These deviations can be attributed to the neglected frequency dependence of ξ_{EH} and ξ_{HE}.

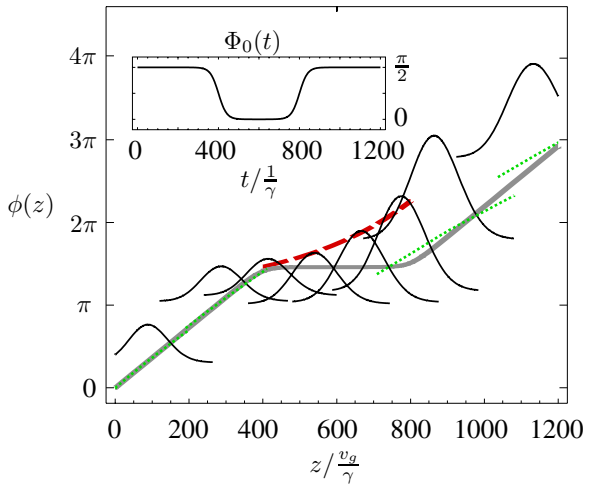

FIG. 3. (Color online) Propagation dynamics in the medium while the closed-loop phase is switched from $\pi/2$ to zero and back to $\pi/2$ throughout the propagation, as shown in the inset. The absolute value (black solid lines) of the probe pulse envelope is plotted for successive propagation times. The scaling and offsets are used as in Fig. 2. At the beginning and at the end of the propagation the spatial phase dependence of each pulse (dashed green straight lines) is compared to the value expected from the analytical solution (thick gray line). During the time period of zero control phase, probe pulse envelope phase does not change and the pulse experiences gain instead, as indicated by the thick dashed red line.

In a second example, the phase Φ_0 is changed during the propagation. Initially, it is set to $\pi/2$ as in the first example. During the course of propagation, it is switched to zero for an intermediate period of time and finally, it is switched back to $\pi/2$. The numerical results for the corresponding propagation dynamics are shown in Fig. 3 and the time-dependent value of the phase is shown as inset in Fig. 3. In the initial and final part of the propagation with phase $\pi/2$, we find the same propagation dynamics as in Fig. 2, with reduced group velocity v_g and with a linear increasing of the phase. But during the period with control phase switched to zero, the phase of the pulse envelope remains approximately constant. Instead, its amplitude increases exponentially. As in the first example, this dynamics can be explained based on the index of refraction at resonance. Calculating β for $\Phi_0=0$ in the analytical solution, we find a negative imaginary value corresponding to gain. Again, we compare the analytical solution to the numerical data. The phase dependence is given by a linear increase with a plateau in between, whereas the increase in amplitude follows an exponential function, see Fig. 3. Both analytical solutions agree reasonably well with the numerical data, given that the finite switch period with the corresponding transient dynamics as well as the frequency dependence of ξ_{EH} and ξ_{HE} is not taken into account in the analytical calculation.

These examples show that by changing the relative control field phase Φ_0, the dynamics of the probe field can be substantially influenced throughout the propagation. In the second example, the refractive index experienced by a pulsed probe field was changed from a positive real value $n \geq 1$ to an imaginary value representing gain and back. With different values for the control phase, also $n \leq 1$, absorption, or intermediate cases are possible. This is illustrated in Fig. 4, which depicts the real and the imaginary part of β obtained from our analytical calculation against the control phase.

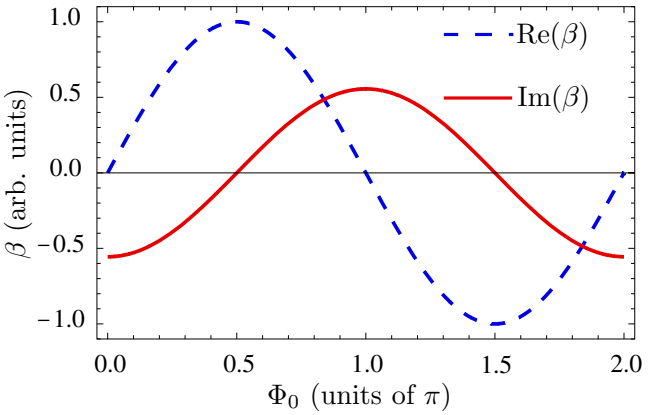

FIG. 4. (Color online) Real (dashed blue line) and imaginary (solid red line) part of β against the closed-loop phase Φ_0.

We conclude by discussing the case of a right-circularly polarized probe field. From Eq. (15), we find that then the response coefficients ξ_{EH} and ξ_{HE} each enter the index of refraction with opposite sign. It follows from Eqs. (24) that this change in sign is equivalent to changing the closed-loop phase by π, i.e., $\Phi_0 \rightarrow \Phi_0 + \pi$. Thus, we conclude that the propagation dynamics presented in Figs. 3 and 4 also hold for right-circularly polarized probe fields provided that the closed-loop phase is shifted by π. It is interesting to connect this result with the observation at the end of Sec. V A that in a certain parameter range the relation $\xi_{EH}=-\xi_{HE}$ as in chiral media can be achieved. This occurs for $\Phi_0=\pm\pi/2$. From Fig. 4 we find that for these values of the closed-loop phase, switching from left-to right-circularly polarized probe field is equivalent to changing the sign of β.

VI. DISCUSSION AND SUMMARY

In summary, we discussed light propagation dynamics in an atomic medium with a cross coupling between the electric and magnetic probe field component. The cross coupling is induced by additional control fields, forming a closed interaction loop. We derived wave equations for both probe field components in the medium and using the slowly varying envelope approximation solved these equations in Fourier space. This solution elucidates the actual dependence of the propagation dynamics on the direct and cross coupling response functions in a macroscopic electrodynamic description. Based on these results, we discussed the general conditions necessary for realizing an atomic medium with a cross coupling. In a concrete example we analytically determined the response functions for a specific model system from the microscopic quantum mechanical EOM. As our main result, we demonstrated that cross couplings can crucially influence the propagation dynamics already at experimentally accessible parameter ranges. As a specific example, we showed that the cross couplings render the medium sensitive to the relative phase of the applied fields. By changing the relative

phase of one of the applied coupling fields, the propagation of a probe pulse can be controlled dynamically during its passage through the medium. The relative phase is independent of the probe field properties and no parametric scattering of coupling fields in to the probe field mode occurs in the absence of the probe field. From this, we concluded that media with a field-induced cross coupling are an ideal implementation of closed-loop phase control of light propagation. The crucial role of the closed-loop phase suggests a possible experimental verification of our results along the line of experiments demonstrating closed-loop configurations with only the electric field component coupling to the medium [29,34,44]. In a broader context, it is remarkable that the magnetic field component of the probe field can substantially modify the probe pulse propagation dynamics, despite the weak coupling of the magnetic field to the medium. The phase dependence is a direct signature of this magnetic coupling in the discussed example. It remains to be seen if such magnetic field couplings may also find other applications in quantum optics.

[1] M. O. Scully and M. S. Zubairy, *Quantum Optics* (Cambridge University Press, Cambridge, 1997).

[2] R. Loudon, *The Quantum Theory of Light*, 3rd ed. (Oxford University Press, Oxford, 2000).

[3] M. Ö. Oktel and Ö. E. Müstecaplıoğlu, Phys. Rev. A **70**, 053806 (2004).

[4] Q. Thommen and P. Mandel, Phys. Rev. Lett. **96**, 053601 (2006).

[5] J. Q. Shen and S. He, Ann. Phys. **16**, 364 (2007).

[6] J. Kästel, M. Fleischhauer, S. F. Yelin, and R. L. Walsworth, Phys. Rev. Lett. **99**, 073602 (2007).

[7] P. P. Orth, J. Evers, and C. H. Keitel, e-print arXiv:0711.0303.

[8] J. Ruostekoski and J. Javanainen, Phys. Rev. A **55**, 513 (1997).

[9] M. Fleischhauer and S. F. Yelin, Phys. Rev. A **59**, 2427 (1999).

[10] O. Morice, Y. Castin, and J. Dalibard, Phys. Rev. A **51**, 3896 (1995).

[11] J. B. Pendry, Science **306**, 1353 (2004).

[12] V. A. Sautenkov, Y. V. Rostovtsev, H. Chen, P. Hsu, G. S. Agarwal, and M. O. Scully, Phys. Rev. Lett. **94**, 233601 (2005).

[13] M. Fleischhauer, Opt. Express **4**, 107 (1999).

[14] A. B. Matsko, I. Novikova, M. O. Scully, and G. R. Welch, Phys. Rev. Lett. **87**, 133601 (2001).

[15] R. Fleischhaker, T. N. Dey, and J. Evers, e-print arXiv:0902.0752.

[16] S. J. Buckle, S. M. Barnett, P. L. Knight, M. A. Lauder, and D. T. Pegg, Opt. Acta (Lond.) **33**, 1129 (1986).

[17] W. Maichen, F. Renzoni, I. Mazets, E. Korsunsky, and L. Windholz, Phys. Rev. A **53**, 3444 (1996).

[18] M. Burresi, D. van Oosten, T. Kampfrath, H. Schoenmaker, R. Heideman, A. Leinse, and L. Kuipers, Science **326**, 550 (2009).

[19] J. D. Jackson, *Classical Electrodynamics*, 3rd ed. (Wiley, New York, 1998).

[20] B. Jungnitsch and J. Evers, Phys. Rev. A **78**, 043817 (2008).

[21] E. Plum, J. Zhou, J. Dong, V. A. Fedotov, T. Koschny, C. M. Soukoulis, and N. I. Zheludev, Phys. Rev. B **79**, 035407 (2009).

[22] It is probably for these analogies that in previous work on NRI media in atomic gases, the cross coupling of the electric and magnetic probe field component was identified with a chiral medium.

[23] E. U. Condon, Rev. Mod. Phys. **9**, 432 (1937).

[24] A. Lakhatakia, V. K. Varadan, and V. V. Varadan, in *Time-Harmonic Electromagnetic Fields*, Chiral Media Lecture Notes in Physics Vol. 335 (Springer, Berlin, 1989).

[25] D. P. Craig and T. Thirunamachandran, *Molecular Quantum Electrodynamics* (Dover, Mineola, 1998).

[26] H. Haken and H. C. Wolf, *The Physics of Atoms and Quanta*, 7th ed. (Springer, Berlin, 2005).

[27] A. J. Flikweert, T. Nimalasuriya, C. H. J. M. Groothuis, G. M. W. Kroesen, and W. W. Stoffels, J. Appl. Phys. **98**, 073301 (2005).

[28] P. P. Orth, Master thesis, University of Heidelberg, 2007.

[29] H. Kang, G. Hernandez, J. Zhang, and Y. Zhu, Phys. Rev. A **73**, 011802(R) (2006).

[30] D. V. Kosachiov, B. G. Matisov, and Y. V. Rozhdestvensky, J. Phys. B **25**, 2473 (1992).

[31] E. A. Korsunsky and D. V. Kosachiov, Phys. Rev. A **60**, 4996 (1999).

[32] G. Morigi, S. Franke-Arnold, and G. L. Oppo, Phys. Rev. A **66**, 053409 (2002).

[33] V. S. Malinovsky and I. R. Sola, Phys. Rev. Lett. **93**, 190502 (2004).

[34] A. F. Huss, R. Lammegger, C. Neureiter, E. A. Korsunsky, and L. Windholz, Phys. Rev. Lett. **93**, 223601 (2004).

[35] H. Shpaisman, A. D. Wilson-Gordon, and H. Friedmann, Phys. Rev. A **71**, 043812 (2005).

[36] S. Kajari-Schröder, G. Morigi, S. Franke-Arnold, and G. L. Oppo, Phys. Rev. A **75**, 013816 (2007).

[37] M. Mahmoudi and J. Evers, Phys. Rev. A **74**, 063827 (2006).

[38] R. Fleischhaker and J. Evers, Phys. Rev. A **77**, 043805 (2008).

[39] W. E. van der Veer, R. J. J. van Diest, A. Donszelmann, and H. B. van Linden van den Heuvell, Phys. Rev. Lett. **70**, 3243 (1993).

[40] A. J. Merriam, S. J. Sharpe, M. Shverdin, D. Manuszak, G. Y. Yin, and S. E. Harris, Phys. Rev. Lett. **84**, 5308 (2000).

[41] S. A. Babin, S. I. Kablukov, U. Hinze, E. Tiemann, and B. Wellegehausen, Opt. Lett. **26**, 81 (2001).

[42] S. E. Harris, Phys. Today **50** (7), 36 (1997).

[43] M. Fleischhauer, A. Imamoglu, and J. P. Marangos, Rev. Mod. Phys. **77**, 633 (2005).

[44] A. F. Huss, E. A. Korsunsky, and L. Windholz, J. Mod. Opt. **49**, 141 (2002).

[45] C. Liu, Z. Dutton, C. H. Behroozi, and L. V. Hau, Nature (London) **409**, 490 (2001).